Microsurgical and 3D anatomy of the male retropubic space and urogenital diaphragm for the future prostatic surgery

Hyun Min Choi

Department of Medicine

The Graduate School, Yonsei University

Microsurgical and 3D anatomy of the male retropubic space and urogenital diaphragm for the future prostatic surgery

Directed by Professor Hye-Yeon Lee

The Doctoral Dissertation submitted to the Department of Medicine, the Graduate School of Yonsei University in partial fulfillment of the requirements for the degree of Doctor of Philosophy

Hyun Min Choi

June 2020

This certifies that the
Doctoral Dissertation of Hyun Min Choi
is approved.

Thesis Supervisor : Hye-Yeon Lee

Thesis Committee Member#1 : Young-Tae Kim

Thesis Committee Member#2 : Ji-Cheol Shin

Thesis Committee Member#3: Jang-Hwan Kim

Thesis Committee Member#4: Hee-Jun Yang

The Graduate School
Yonsei University

June 2020

ACKNOWLEDGEMENTS

I would like to express the deepest appreciation to Professor Hye-Yeon Lee, who continually and convincingly conveyed a spirit of adventure in regard to research and scholarship. Without her guidance and persistent help this dissertation would not have been possible.

I would like to thank my committee members, Professor Young-Tae Kim, Professor Ji-Cheol Shin, Professor Jang-Hwan Kim, and Professor Hee-Jun Yang, who embodied the figure of a kind professor, provided maximum support and instilled enthusiasm in regards to my research.

Greatest thanks to Yeong-Kil Kang, So-Young Jung, Soo-Jung Kim who spent their late hours for assisting me with experimentation and kindly provided critical revision of the photos and the results of the experimentation.

Finally, I give my special thanks to my parents and parents-in-law for their tremendous support. I also express my fondest appreciation and love to my wife Woo-Jin and to my beloved daughter Ji-An. Their unfailing love enabled me to complete this work.

by Author

<TABLE OF CONTENTS>

LIST OF FIGURES

LIST OF TABLES

ABSTRACT

Microsurgical and 3D anatomy of the male retropubic space and urogenital diaphragm for the future prostatic surgery

Hyun Min Choi

Department of Medicine
The Graduate School, Yonsei University

Directed by Professor Hye-Yeon Lee

Introduction: The anatomical and functional importance of the puboprostatic c ligament (PPL) is increasingly recognized as essential to prevent complications of urinary incontinence and erectile dysfunction following radical prostatectomy. The Retzius-sparing technique was recently introduced as a method to preserve the PPL and neurovascular bundles. Detailed understanding of the precise anatomy of the PPL and its variations, and the neurovascular bundle, proximal urethra, prostate, and surrounding structures is imperative for both surgical planning and subsequent reconstruction to preserve urinary continence and erectile function. However, despite greatly affecting surgical outcomes, due to the difficulty of microanatomic study in these small and variable perineal muscles, there are few papers detailing the basic anatomy of the retropubic space. We conducted this study to further understanding of the anatomic variations of the PPL and perineal muscles in the retropubic space. We also conducted a three-dimensional (3D) computed tomography (CT) scanning image study using Lugol's solution and compared reconstructed images with real samples.

Materials and Methods: Cadavers of 30 Korean men who had not undergone surgery in the relevant areas, donated to Yonsei University College of Medicine, were used in this study. In each case, the pelvis was dissected using a conventional technique to observe the PPL. The superficial perineal pouch, perineal body, and deep perineal pouch were dissected for observation of their anatomical structures. Six samples stained with Lugol's solution were scanned using a conventional CT system. Images were reconstructed into 3D images for comparison with the actual dissection. For statistical analyses, Student's t-test and chi-square test were used.

Results: Depending on the site of attachment, PPLs mostly (54.7%) had a linear form (Type I). Type II PPL and Type III PPL, which are connected to the tendinous arch were also observed. In some samples it was quite challenging to classify the type. Two PPLs were observed in 25% of all samples. The location of the attachment of the PPLs to the pubis was very deep in the lower third of the pubic bone. The medial border of the PPL was attached to a point which was, on average, 3.5 mm from the inner margin of the pubic body; while the lateral border was attached to a point, on average, 8.5 mm from the pubic body. In cases with more than two ligaments on one side, the distance between the bilateral ligaments was shorter than average. The 'cutaneous central band' in the perineum was observed to connect the bulbospongiosus muscle (BSM) and cutaneous external anal sphincter. The cutaneous central band was a narrow and deeply formed band of fibrous tissue. The fibrous band of the BSM that connects to the median raphe was observed to connect to the cutaneous fibers of the anal sphincter. The accessory superficial perineal muscle, which is located closer to the surface than the perineal membrane, was found in 61.5% of all samples.

The perineal body consists of superficial and deep layers. The muscles within the deep perineal pouch were not in the form of a fascia with the muscles aligned

in a horizontal fashion, but were hoof shaped (similar to the anatomy of the female compressor urethra muscle). The anterior side of the urethra was either short or wide. In cases of urethra with a wide anterior side, muscle fibers were also observed around the anterior.

Three-dimensional reconstruction of CT scans of the muscles of the urogenital diaphragm revealed individual layers and patterns of the shallow layers which were able to be visualized and analyzed in detail on the 3D images. However, because the muscles in the deep layers were thin and exhibited various patterns, clear observation of their structure on the 3D images was limited.

Conclusions: PPLs exhibited various morphologies which were classified into four different types based on the attachment type: Type I, which connects linearly from the pubic bone to the prostate, accounted for 54.7% of cases. Type II, which starts from the pubic bone and attaches to the prostate and prostate, tendinous arch, accounted for 37% of cases. Type III, which occurs when the ligaments from the pubic bone and the tendinous arch combine and attach to the prostate, accounted for 6.7% of cases. Type IV is characterized by multiple ligaments arising from the pubic bone to form a complex structure. Two PPLs were observed in 25% of all samples. The PPL was attached to the pubis very deep in the lower third of the pubic bone. The medial border of the PPLs attached to a point, on average, 3.5 mm from the inner margin of the pubic body, while the lateral border attached to a point, on average, 8.5 mm from the pubic body. In cases with more than two ligaments, the distance was shorter than the average. The fibrous connecting band between the anus and bulbar was observed superficially. This cutaneous central band was narrow and deeply formed with fibrous tissue. The fibrous band of the BSM that connects to the median raphe was observed to connect to the cutaneous fibers of the anal sphincter. The accessory superficial perineal muscle, which is located closer to the surface than

the perineal membrane, was observed in 61.5% of all samples.

The perineal body consists of superficial and deep layers. The muscles within the deep perineal pouch were not observed in the form of a fascia with the muscles aligned in a horizontal fashion but were hoof shaped (similar to the female anatomical structure of the compressor urethra muscle). The anterior side of the urethra was either short or wide. In cases with a urethra with a wide anterior side, muscle fibers were also observed around the anterior.

Three-dimensional reconstructions of CT scans of the muscles of the urogenital diaphragm were performed. During image analysis, individual layers and patterns of the shallow layers were visualized and analyzed in detail on the 3D images. However, because the muscles in the deep layers were thin and exhibited various patterns, clear observation of their structure on the 3D images was limited.

Key words: prostate cancer; puboprostatic ligament; urogenital diaphragm; 3D anatomy

Microsurgical and three-dimensional anatomy of the male retropubic space and urogenital diaphragm for the future prostatic surgery

Hyun Min Choi

Department of Medicine
The Graduation School, Yonsei University

(Directed by Professor Hye-Yeon Lee)

I. INTRODUCTION

The incidence of prostate cancer has been increasing sharply in Korea[1] since the introduction of early prostate-specific antigen (PSA) screening in 1990, along with the recent adoption of a western style diet. The most common treatment for organ-confined prostate cancer is radical prostatectomy (RP). Retropubic RP was introduced at the beginning of the 1900s. The major morbidities of this procedure are urinary incontinence and erectile dysfunction.[2,3] Post RP incontinence is reported by around 30% of patients, and takes at least two years to stabilize.[4,5] After its introduction in 2001, robot assisted laparoscopic radical prostatectomy (RALRP) became the gold standard for prostatic cancer surgery. As proposed in 2005, the trifecta (cancer free, potent, and continent) and has become the optimal outcome that urologists seek to achieve following RALRP.[6] Thereafter, various surgical techniques have been used. Robot assisted surgical techniques were developed including infrafascial neurovascular bundle saving[7], membranous urethra maximization[8], bladder neck preservation[9], bladder neck

reconstruction[10], posterior reconstruction[11], anterior retropubic suspension[12], and lateral prostatic preservation[13].

A study comparing the surgical results of open RP and RALRP reported no differences in oncologic outcomes, but functional outcomes of incontinence and erectile dysfunction were better following robot surgery.[14] While perineal RP allows more precise dissection of the urethra and spares the Retzius space and dorsal vein complex (DVC), it damages the pelvic floor musculature and may lead to high rates of incontinence. By contrast, causing more surgical trauma to the puboprostatic ligament (PPL), neurovascular bundle, and endopelvic fascia. Galfano et al developed a new Retzius-sparing approach through the pouch of Douglas which avoids all the Retzius structures: the Santorini plexus, PPL, endopelvic fascia, and neurovascular bundles. They report the Retzius-sparing approach to be oncologically safe and result in high early continence and potency rates.[15,16] Lim et al also validated the excellent oncological and continence outcomes of Retzius-sparing approach and reported that although technically more demanding, this approach was as feasible and effective as conventional RALPR, and also led to shorter operating time and faster recovery of continence.[17] There is great variation in prostate size, shape, and surrounding fascia, ligaments, and neurovascular bundle. These variations affect surgical outcomes greately.[18-20] It is surprising how little is known about the anatomy of the puboprostatic ligament (PPL) which connects the pubic bone and prostate, and supports the prostatic urethra. In their report of the Retzius-sparing technique, Galfano et al did not detail the surgical and functional anatomy of the PPL and its various anatomic variations.

Some patients experience dual problems of urinary incontinence and erectile dysfunction following RP of various techniques. Choi et al reported implanting a three-piece inflatable prosthesis in patients with dual problems of erectile

dysfunction and incontinence after RP. They indicated very promising results, including curing incontinence in 72% of patients.[21] During robot surgery, if the patient has unexpected anomalous variations of anatomy, blunt dissection may lead to injury of the PPL and the DVC, resulting massive bleeding. These unexpected unfavorable outcomes usually result from the surgeon's poor knowledge of the variations of the PPL and related retropubic anatomy. Even in cases of successful RALRP, stress incontinence may occur due to injury of the PPL, neurovascular bundle (NVB), supporting pelvic fascia, and pelvic floor muscles. Urologically, the PPL is the most important supporting structure in the retropubic space. Thus, it is surprising how little is known about its anatomy. Most existing anatomic accounts of the PPL are inaccurate and lack extensive study of its variations.

Steiner performed a detailed anatomic study of the PPL and male urethral suspensory mechanism by anatomic dissection of the male cadaver. He reported that the PPL was not a discrete "band" of fascia but a pyramid shaped structure that is part of a larger urethral suspensory mechanism that attaches the membranous urethra to the pubic bone. He classified PPLs as anterior, middle, and posterior. Steiner maintained that if dividing the PPL is necessary during surgery, preservation of the anterior and middle PPL is necessary to prevent incontinence.[22] Kim et al dissected six cadavers and analyzed the surgery videos of 300 RALRP and classified the PPL into four types.[23] Clinicians insist that they can preserve the PPL and NVB, but there are no published clear cut explanations for how the procedure is performed.

As radical pelvic surgery continues to advance, a better understanding of the precise anatomy of the proximal urethra, prostate, PPL, and surrounding structures is imperative for both surgical planning and subsequent reconstruction, to preserve urinary continence and erectile function. One

advantage of laparoscopic and robotic technology, is the investigation of spaces and anatomical recesses which can provide important, solid, and detailed basic anatomic knowledge in the field of urology.

To prevent unexpected problems during RP and reduce post-surgical complications, here we present the results of an extensive basic anatomic study of the morphology, types, size, location, and variations of the PPL. We also report variations of the superficial and deep perineal muscles of the urogenital diaphragm.

The reasons for the controversial reports about the urogenital diaphragm, appear related to the difficulty of an anatomic approach and a limited numbers of samples.[24] Studying the microanatomy of the muscles such as the perineum with a small number of cases and large variations is very challenging. We stained six samples with Lugol's solution which has previously only been used in animal studies. We then obtained computed tomography (CT) scans of the samples. The CT scans were then reconstructed into three-dimensional (3D) images. We investigated whether this procedure could replace histological analysis of human skeletal muscles and actual dissection for studying the muscle layers. We tested the feasibility of developing future virtual training models.

II. Materials and Methods

1. Materials

We used the pelvises from thirty Korean male cadavers donated to Yonsei University College of Medicine. We excluded samples that had undergone surgery in the pelvic region. The mean age of the cadavers was 79.6 years (61–96 years). Sixteen specimens were student education cadavers which had been embalmed with formalin as per routine. The thirteen specimens were fresh frozen cadavers which were defrosted and fixated in 10% formaldehyde mixture;

these were used for studying the anatomy of PPL and the perineal structures. Six fresh frozen cadaver pelvises were processed with Lugol's staining for CT radiography and analysis. One specimen that had undergone soft embalming using salts was studied for observation of surgical anatomy.

2. Methods

A. Cadaver fixation

(A) Formalin fixation

In accordance with the usual method for fixation of an anatomical cadaver, cadavers were perfused with a 10% formalin solution via the femoral artery and kept for one year before use.

(B) Fixation of frozen cadavers

After defrosting fresh frozen cadavers, pelvises were isolated and soaked in 10% formalin and 70% alcohol mixture for 10 days.

(C) Soft embalming

One cadaver was embalmed with a saturated salt solution1 and kept refrigerated for six months. The soft embalmed cadaver was used to review surgical techniques.

B. Lugol's staining

Samples that had been fixated with 10% formalin were washed with water for one day. The deep perineal pouch and urogenital diaphragm were injected with 0.5 ml of 100% Lugol's solution (iodine potassium iodide solution), in 4 cm2 intervals. The samples were immersed in Lugol's solution (25%) for three weeks. During this time, the immersion solution was changed twice per week.

C. Intravenous silicon injection

After making an incision in the skin over the penile dorsum, blue silicone (MICROFIL, Flow Tech, MA, USA) was injected into the deep dorsal penile vein. After checking the filling of the silicone into the internal iliac vein, it was tied. A sufficient amount of silicone was injected into the prostatic plexus.

D. Dissection

For investigation of the anatomy of the puboprostatic ligament, an incision was made in the endopelvic fascia anterior to the bladder, and the retropubic space was dissected. First, the position and tributaries of the dorsal vein of the penis were identified, and the puboprostate ligament was observed. To secure sufficient space for observation, the attachments of the levator ani muscle to the mid-point of the sacrum and the tip of the coccyx were preserved. Part of the pelvis posterior to the ischial tuberosity was removed to enable observation of the local anatomical relations in the retropubic space.

After removing the skin over the perineal region, the superficial anal sphincters, superficial transverse perineal muscle, and the bulbocavernosus muscle (BCM) were dissected, and the alignment of the muscle fibers was observed. After verifying the urogenital diaphragm of the BCM, connection of the BCM with the external urethral sphincter was examined. The presence or absence of structures that form the perineal body was also noted.

After identifying the structures of the superficial perineal pouch, the crus of the penis were separated from the ischium, and the corpus spongiosum was separated from the pubic bone to expose the urogenital diaphragm. The bulb and muscles were left in place so the relationship between the transverse perineal muscle and the perineal body in the deep layer could be verified. The perineal

membrane was removed, and the alignment of the muscle fibers of the deep transverse muscle, external urethral sphincter, BCM, and anal sphincter were observed. The presence or absence of the longitudinal rectourethral muscle attached to the perineal body was noted, and if present, its position was noted. All dissections were performed with precision, using a 4× magnification surgical microscope when necessary.

After observing the urogenital diaphragm, the structures surrounding the prostatic venous plexus were separated from the prostate apex, and the space between the apex and urogenital diaphragm was cleared. The urethra at this location was observed and its length was measured, before confirming the absence of the apron.

In some samples, a mid-sagittal section was taken centered on the urethra. This was used to observe the relationship of the membranous urethra with the surrounding structures and to observe and compare the positions of the urogenital diaphragm, prostate, tendinous arch, and surrounding structures.

E. Analyzing the morphology and position of the puboprostatic ligament

(A) Morphological classification

The appearance, shape, and angle of the puboprostatic ligament were observed where it attaches to the pubic bone. In addition, it was classified into one of three types based on whether the ligament was attached or connected to the tendinous arch. The number of puboprostatic ligaments was also verified, and the positions of the dorsal vein of the penis and the ligaments were observed.

(B) Measurement of size and position

The width of the ligament attachments were measured, including the parts toward the middle where the size changed. The vertical distance of the

attachment to the pubic bone from the most superior edge of the bone, and from the medial edge to the lateral edge were measured. The space between the two ligaments was measured as the distance between the two attachments.

F. Structure and measurement of the urogenital diaphragm

1) Observed the existence and shape of superficially located muscles over the perineal membrane and their relationship with the bulbocavernosus muscle.
2) Observed the composition of the perineal body and its relationship with the anal sphincter.
3) Measured the length and width of the superficial transverse perineal muscle, the length of the attachment of the bulbospongiosus muscle (BSM), the distance between the center of the perineal body and the anterior border of the anus, and the length and breadth of the urogenital diaphragm.
4) Observed the arrangement of the deep perineal muscle and the course of the neurovascular bundle in the deep perineal pouch and verified the existence of the compressor urethra.
5) Established the anatomy of the retropubic space.

G. 3D remodeling of the perineal muscle

Lugol stained samples were imaged at 140 kV using a conventional CT system (Revolution CT, GE Healthcare, Milwaukee, WI). Digital imaging and communications in medicine (DICOM) images were reconstructed in 3D using OsiriX Lite software (Pixmeo SARL, Bernex, Switzerland). Colors were assigned according to each image index for differentiating the muscle, bone, and connective tissue. After cropping unrelated structures, a 3D image was made

and each transverse slice was analyzed at the required angle to observe individual layers (Figure 1).

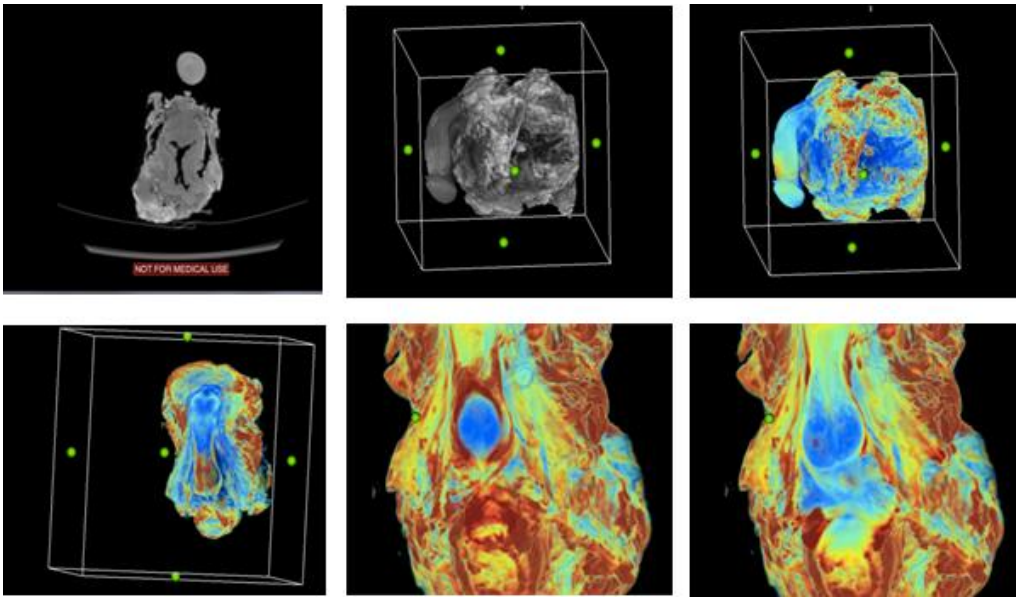

Figure 1. Three-dimensional (3D) reconstruction process. From upper left to lower right side, the process of using CT DICOM image to create 3D reconstructed and colored images. changed the dimension to find the structure.

H. Statistical analysis

All data were analyzed using Student's t-test, and frequencies were analyzed using the chi-square test.

III. RESULT

1. Anatomy of puboprostatic ligament

A. Number and Shape

PPLs were observed in all samples (Table 1), except for one which showed no PPL on the left side. No difference in the number of PPLs was observed between the right and left sides. A total of 64 ligaments were observed. In a single sample, the number of PPLs tended to be symmetrical. One PPL was observed on each

side (left and right) in 61.5% of samples, and two PPLs on each side were observed in 15.4% of samples. Two PPLs were observed in 25% of all samples. The number of PPLs were different between both sides in 19.2% of the samples.

Table 1. Number of PPL

Number	Right (n=26)	Left (n=26)	Total (n=52)
0	0.0%	3.9%	1.9%
1	73.1%	73.1%	73.1%
2	26.9%	23.1%	25.0%
Total	100.0%	100.0%	100.0%

PPL, puboprostatic ligament

PPLs exhibited various morphologies which were classified into four different types based on the type of attachment (Table 2). Type I PPLs, which connect linearly from the pubic bone to the prostate, accounted for 54.7% of all samples. Type I PPLs included type Ia PPLs, which are deep and narrow; and type Ib PPLs, which are wider and shallow (Figure 2.). Both subtypes were observed at similar proportions. Type II PPLs, which start from the pubic bone and attach to the prostate and tendinous arch, were observed in 37.0% of all samples. Type II PPLs are classified as type IIa, which has a single attachment to the prostate; and type IIb which has a double (or more) attachment to the prostate. Most type II PPLs were observed to attach widely to the prostate as a whole (Figure 3). Type III PPLs, which occur when the ligament from the pubic bone and the ligament from the tendinous arch combine and attach to the prostate, were observed in 6.7% of all samples. A type IV PPL, which is characterized by multiple ligaments arising from the pubic bone that combine in the middle to form a complex structure, was observed in one sample. No

difference in morphology was found between the right and left sides in all samples (Table 2).

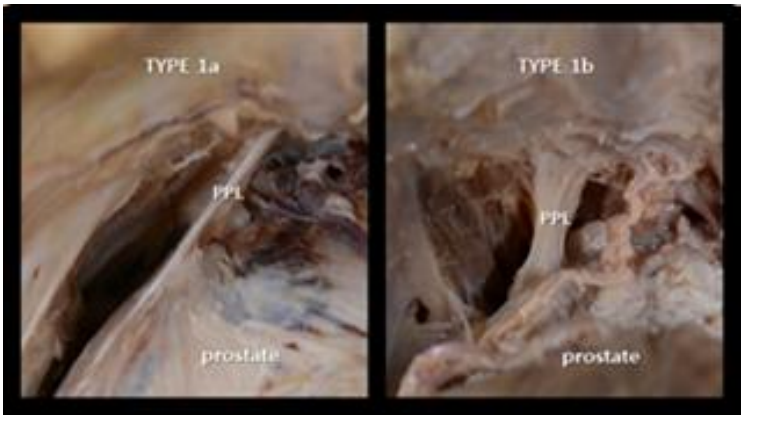

Figure 2. Photograph of straight band shaped type I puboprostatic ligament (PPL). Left; type 1a PPL (narrow and deep attachment). Right; type Ib PPL (wide and shallow attachment). All photos were taken from the left side.

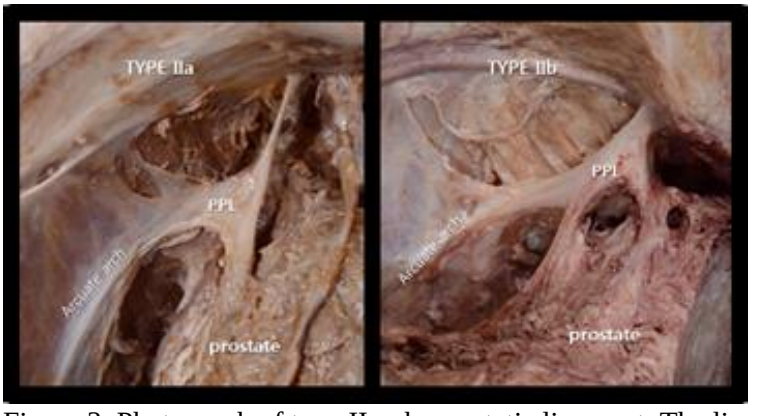

Figure 3. Photograph of type II puboprostatic ligament. The ligament has an accessory slip to the arcuate arch. Left; type IIa PPL (single prostatic attachment). Right; type IIb PPL (double prostatic attachment). All photos were taken from the left side.

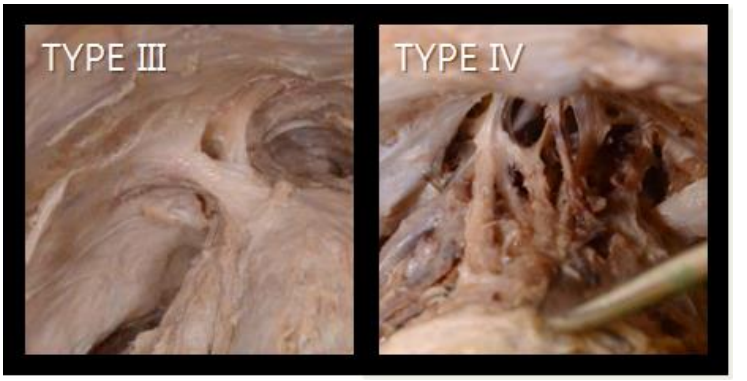

Figure 4. Photograph of type III PPL and type IV PPL. Left; type III PPL has an assistant fiber from the arcuate arch which reinforces the prostatic attachment. Right; type IV PPL has a complex shape. All photos were taken from the left side.

Table 2. Incidence of PPL type

Shape	Right (n=33)	Left (n=31)	Total (n=64)
Type I	54.6%	54.8%	54.7%
Ia	*30.3%*	*25.8%*	*28.1%*
IIb	*24.2%*	*29.0%*	*26.6%*
Type II	39.4%	35.5%	37.5%
IIa	*30.3%*	*25.8%*	*28.1%*
IIb	*9.1%*	*9.8%*	*9.4%*
Type III	6.0%	6.5%	6.3%
Type IV	0.0%	3.2%	1.6%
Total	100.0%	100.0%	100.0%

PPL, puboprostatic ligament

We analyzed the symmetry of the PPL morphology between the left and right sides and investigated whether it changed depending on the number of ligaments. While samples with a single ligament tended to have a greater number of type II PPLs, samples with two PPLs exhibited an increased proportion of type I PPLs (Table 3.). Further analysis based on the number of ligaments on both sides showed that the probability of identical PPL morphology on both sides was 50% (Table 4.).

Table 3. Type of PPL according to the number of ligaments

Type	Single (n=38)	Double (n=26)	Total (n=64)
I	42.1%	73.1%	54.7%
II	44.7%	26.9%	37.5%
III	10.5%	0.0%	6.3%
IV	2.6%	0.0%	1.6%
Total	100.0%	100.0%	100.0%

PPL, puboprostatic ligament

We then compared the morphology of PPLs on the inner side with that of PPLs on the medial and lateral sides using samples with double PPLs. All PPLs on the medial side were type I. Analysis of the symmetricity of morphology showed a higher tendency for identical morphology on both sides for samples with one PPL only, and the rate of identical morphology on both sides tended to be higher in samples with type II PPLs, compared with type I PPLs. Samples with unilateral double PPLs or bilateral double PPLs exhibited various types of PPLs (Table 4.).

Table 4. Symmetricity of number and shape of PPL

Pattern of the ligament number	PPL type (One side / Other side)	Number
Missed ligament on the Lt side	- / II	1
Single ligament on each side	II / II	6
	I / I	4
	I / II	3
	I / III	1
	III / IV	1
	III / III	1
Single and double ligaments	I / I + I†	2
	I / I +II	2
	II / I + II	1
Double ligaments on both sides	I + I / I +II	2
	I + I / I + I	1
	I +II / I +II	1

†For samples with double ligaments, medial PPLs are shown first, followed by lateral PPLs.
PPL, puboprostatic ligament

B. Size

The average breadth of the PPLs was 3.63 mm for the pubic attachment and 6.08 mm for the mid-portion. The breadth of the attachment to the prostate gland was 6.91 mm, which increased toward the pubis. No difference in breadth was found between the left and right (Table 5).

Table 5. Breadth of PPL

Measuring site	Right(mm) (n=33)	Left(mm) (n=31)	Total(mm) (n=64)
Attachment to the pubis	3.78 ± 1.69[1] (0.8-8.9)[2]	3.48 ± 2.04 (0.6-8.6)	3.63 ± 1.86 (0.6-8.9)
Midpoint	6.01 ± 3.25 (2.0-16.9)	6.15 ± 3.53 (1.9-14.0)	6.08 ± 3.36 (1.9-16.9)
Attachment to the prostate	6.81 ± 4.56 (1.5-16.2)	7.02 ± 4.84 (2.5-27.1)	6.91 ± 4.67 (1.5-27.1)

[1]Mean ± standard deviation
[2]Range
PPL, puboprostatic ligament

Comparison of ligament size according to morphology showed no difference in breadth according to the ligament type of the pubic attachment. The breadth of the prostatic attachment was greater for types II and III PPLs than for type I PPLs, without significance. Type II PPLs were observed to be wide in the middle (Table 6). While no change in size of PPL was associated with the number of PPLs, the lateral ligaments were wider than the medial ligaments.

Table 6. Comparison of breadth between PPL type

Site	Type I(mm) (n=35)	Type II(mm) (n=24)	Type III(mm) (n=4)
Attachment to the pubis	3.57 ± 1.83	3.93 ± 1.95	3.06 ± 1.68
	(0.8-8.6)	(1.0-8.9)	(0.6-4.2)
Midpoint	4.85 ± 2.46	8.01 ± 3.58*	5.82 ± 4.37
	(1.9-10.5)	(3.2-16.9)	(3.2-12.4)
Attachment to the prostate	6.19 ± 3.62	8.02 ± 5.65	7.51 ± 5.04
	(1.5-16.2)	(2.2-27.1)	(2.9-12.1)

*Type I vs II mid-point, $p<0.05$
PPL, puboprostatic ligament

C. Location of the pubic attachment

Locations of the attachment of the PPLs to the pubis were observed as follows: The medial border of the PPLs were attached to a point 3.5 mm, on average, from the inner margin of the pubic body. The lateral border attached to a point 8.5 mm, on average, from the pubic body. The distance from pubic body to the lateral border did not exceed 22.4 mm. The pubic attachment was 40.41 (32.0-58.4) mm, on average, beneath the upper pubic margin. For samples with double ligaments, the lateral attachment was located above the medial attachment. No

difference in location was observed between the left and right sides (Table 7).

Table7. Distance of pubic attachment of PPL

Distance	Rt(mm) (n=33)	Lt(mm) (n=31)	Total(mm) (n=64)
From the medial end of the pubic body			
to the medial border of the ligament	3.75 ± 2.12 (0-7.9)	3.25 ± 1.61 (0-7.3)	3.51 ± 1.88 (0-7.9)
to the lateral border of the ligament	8.83 ± 4.53 (2.7-14.2)	8.16 ± 3.03 (2.5-22.4)	8.50 ± 3.82 (2.5-22.4)
From the upper pubic margin			
to the upper border of the ligament	41.17 ± 4.78 (34.8-58.4)	39.61 ± 3.93 (32.0-48.4)	40.41 ± 4.42 (32.0-58.4)

PPL, puboprostatic ligament

D. Distance between the ligaments on the left and right sides

The mean interpubic distance between the ligaments on the left and right was 8.3 (3.18-7.79) mm, and the mean interprostatic distance was 14.0 (3.97-25.19) mm. The distance between the ligaments on the left and right was significantly shorter in samples with double ligaments on either side than in the samples with a single ligament on both sides (Table 8).

Table 8. Distance between bilateral ligament according to number of the of ligaments

	Both single(mm) (n=16)	Either double(mm) (n=5)	Both double(mm) (n=4)
Interpubic distance	9.63 ± 2.81 (5.38-14.89)	5.82 ± 2.05* (3.18-7.88)	6.39 ± 0.93* (5.32-7.36)
Interprostatic distance	14.46 ± 6.11 (4.86-25.19)	13.65 ± 6.95 (5.88-23.01)	12.53 ± 4.75 (7.28-18.62)

* 1 + 1 vs. 1 + 2 , 1 + 1 vs. 2 + 2, $p<0.05$

2. Anatomy of Perineal muscle

A. Cutaneous central band

The fibrous band connecting band was observed to be superficial in the cutaneous tissue between and anus and the bulba. The cutaneous band was narrow and deeply formed with fibrous tissue. While the muscle of the cutaneous anal sphincter was extended for a short distance, it was mostly composed of fibrous tissue. The fibrous band of the BSM connected to the median raphe connected to the cutaneous fiber of the anal sphincter. The thickness of the fibrous band varied between samples (Figure 5).

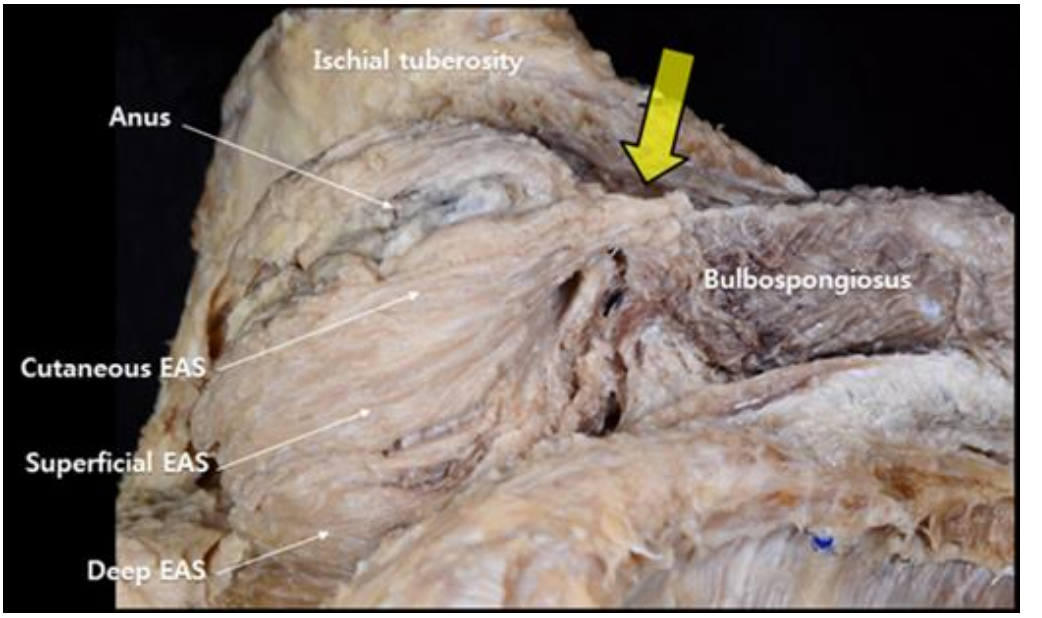

Figure 5. A photography of the cutaneous central band: Large arrow shows cutaneous central band; Each part of the External anal sphincter (EAS) are pointed with long slender arrow.

B. Superficial transverse perineal muscle (STPM)

The superficial transverse perineal muscle (STPM) was observed in almost all samples. Muscles in the form of thin membranes were observed in 16.7% together with accessory muscles. Most of these muscles started from the anterior portion of the ischial tuberosity and joined the bulbar fiber of the BSM in the

middle. In several samples, these muscles connected with the fibers of the superficial anal sphincter (Figure 6). In one sample, the fibers on both sides of the STPM were elongated into a single fiber. In another sample, the STPM bundle extended to the bundle of the superficial anal sphincter past the middle portion. The samples without STPMs had accessory muscles, which are described below.

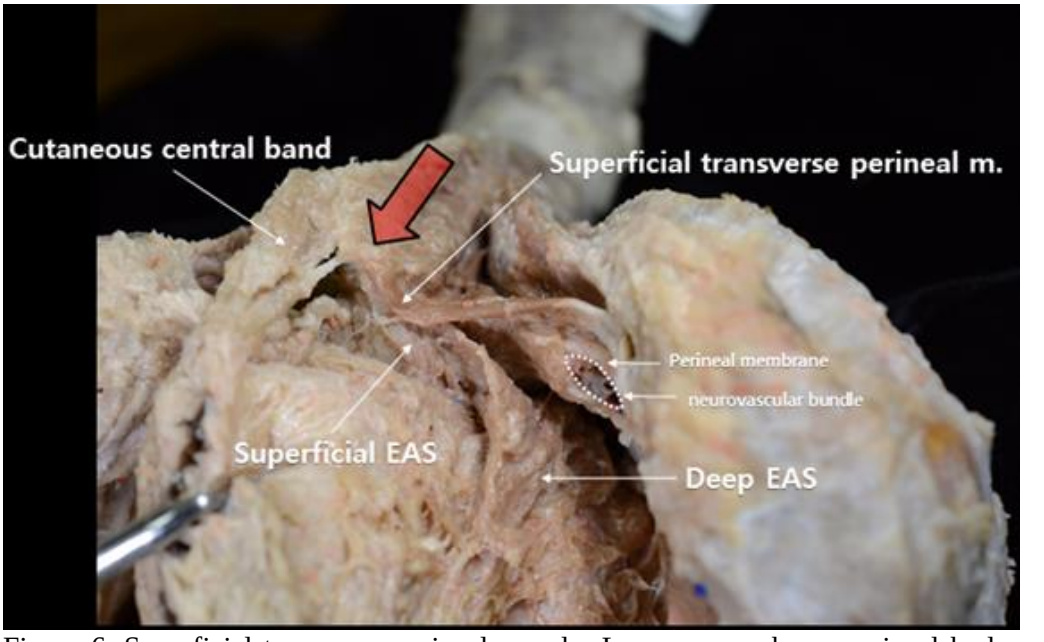

Figure 6. Superficial transverse perineal muscle; Large arrow shows perineal body; External anal sphincter (EAS)

C. Accessory superficial perineal muscle

The accessory superficial perineal muscle was observed to be located closer to the surface than the perineal membrane. It started from the ischium and connected to the BSM. The accessory superficial perineal muscle was found in 61.5% of all samples and were more frequently observed to occur bilaterally (38.4%) than unilaterally (23.1%). The morphology and location of attachment of the accessory superficial perineal muscle varied between samples. The

oblique, band shaped accessory muscles may be hidden by the ischiocavernosus muscle (ICM) and may be confused with the ICM. However, in our samples they were observed to extend toward the lateral side of the distal portion of the BSM and could be clearly distinguished from the ICM (Figure 7).

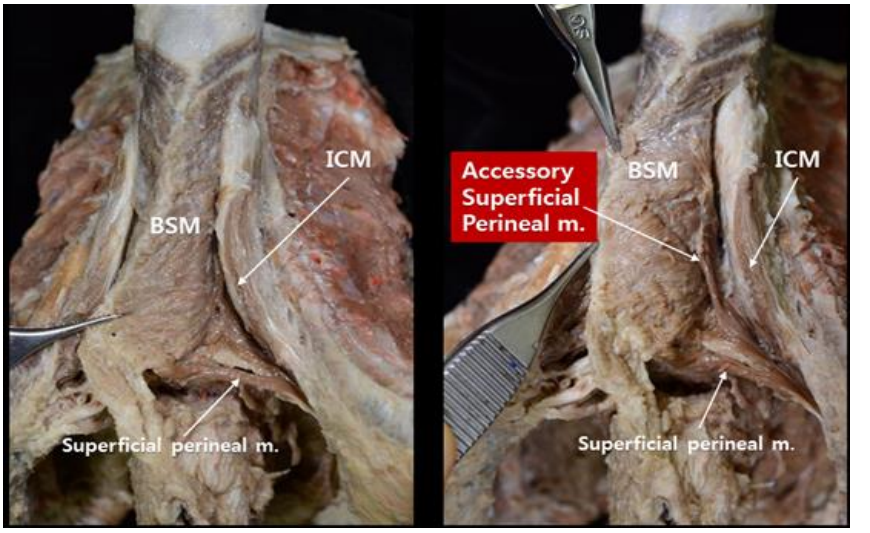

Figure 7. Photograph of accessory superficial perineal muscle. The accessory superficial perineal muscle can be clearly distinguished between the bulbospongiosus muscle (BSM) and ischiocavernosus muscle (ICM). It attaches to the distal part of the BSM in the form of a fan.

Most of the accessory superficial perineal muscles were band shaped diagonally (61.5%) (Figure 8A). They started from the ischial tuberosity to form a triangle and either attach to the bulba and BCM (15.4%; Figure 8B) or connected to the STPM through a slip extending from the diagonal band (15.4%, Figure 8C). In one sample, a triangular accessory muscle was observed to wrap widely around the ventral side of the BSM and connected to the median raphe (Figure 8D).

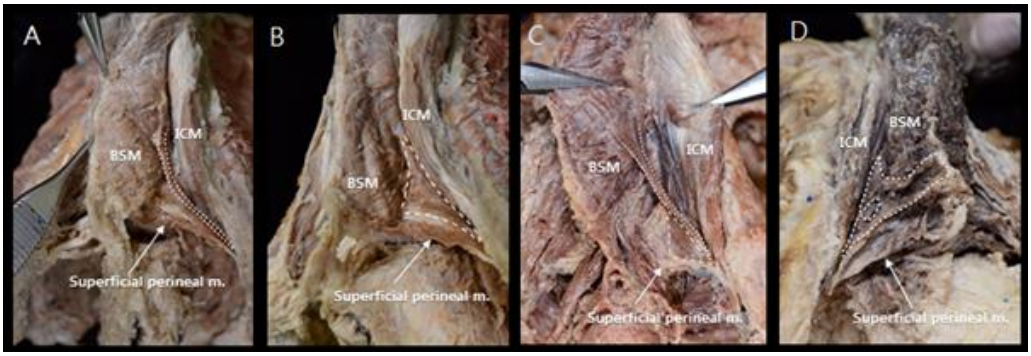

Figure 8. Photographs of types of accessory superficial perineal muscles: (A) Oblique, band shape (61.5%). (B) triangular shape formed by wide connection of the accessory superficial perineal from the ischial tuberosity to the superficial transverse muscle (15.4%). (C) combination of band and triangular shapes (15.4%). (D) triangular shape wrapping around the bulbospongiosus median raphe (7.7%). BSM, bulbospongiosus muscle; ICM, ischiocavernosus muscle.

D. Bulbospongiosus muscle (BSM)

The bulbar muscles were observed to touch the raphe of the dorsal side or the perineal body. In 11.5% of all samples, the BSM was not aligned side-by-side and did not cover the entire bulbar fiber. In some samples, the BSM connected to the fibers of the superficial external anal sphincter. The muscle surrounding the penile shaft was solidly attached to the perineal membrane. In 50% of samples, the accessory superficial perineal muscle fiber traveled sideways to join the bulbar surface at the distal portion of the shaft.

E. Dimension and size of the superficial structures of the urogenital area

The mean distance from the posterior end of the bulbar fiber to the anterior border of the anus was 15.76 ± 16.82 mm. The mean length of the superficial transverse muscles in the relaxed state was 33.6 mm on the left and 38.6 mm on the right. The mean width of the middle part of the bulbar fiber was 2.2 mm on the left and 1.5 mm on the right. The mean length of the accessory superficial muscles was 35.61 mm, and the mean vertical height of the proximal site from

the end of the bulbar fiber was 20.5 mm.

The mean length of the mid-portion of the BCM was 44.8 mm on the median side and 55.47 mm on the lateral side, which was 10 mm longer than the length of the former. The total mean length was 56.8 (41.5-75.0) mm on the right and 55.6 (41.3-72.8) mm on the left; the mean length was greater on the right without significance. The mean width of the bulbar fiber attached to the muscle was 27.7 mm (Figure 9).

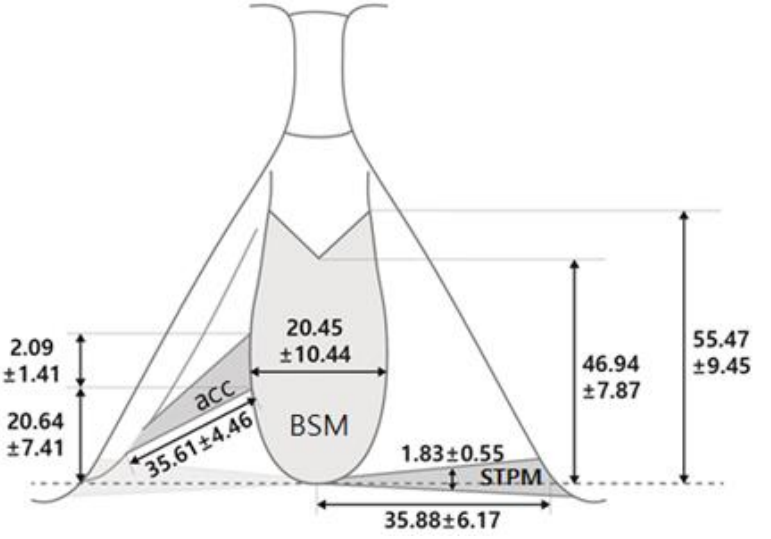

Figure 9. Dimension of the superficial perineal muscle. BSM, bulbosponsiosus muscle; STPM, superficial transverse perineal muscle; acc, accessory superficial transverse perineal muscle

F. Composition of the perineal body

The perineal body was divided into where the muscles of the shallow layers were attached, and where the muscles of the deeper layers were attached. In the muscles of the shallow layers, the connection between the deep fiber transverse perineal muscle of the BSM, STPM, and superficial anal sphincter, and the deep anal sphincter were observed. The point at which the muscles of the deep layers were combined was more superior and anterior than the point at which the muscles of the shallow layers met (Figure 10). In some samples, the muscle

fibers of the superficial perineal muscle and the superficial anal sphincter crossed one another and connected (Figure 11).

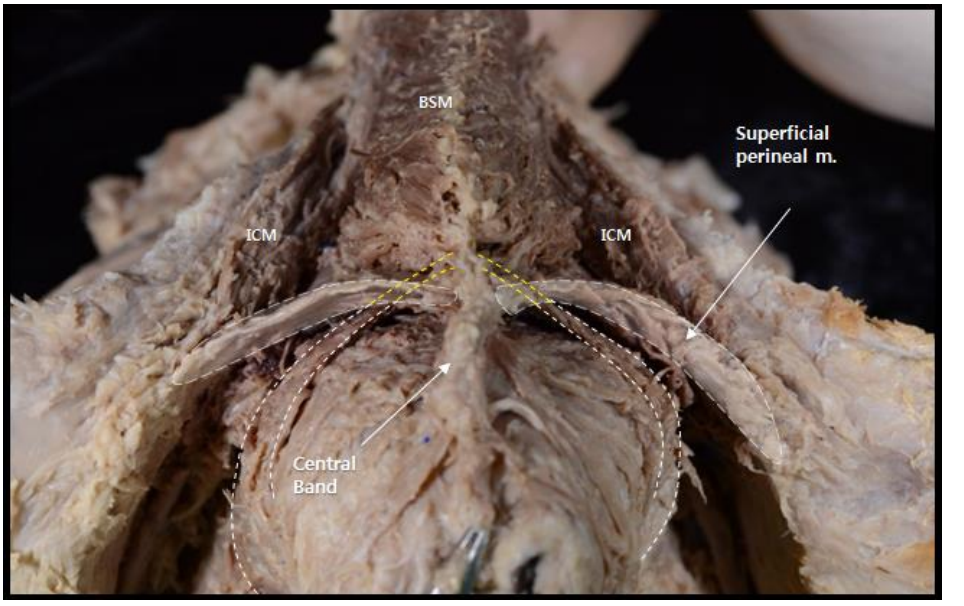

Figure 10. Photograph of the layers of perineal body: Ischiocavernosus muscle (ICM); Bulbosponsiosus muscle (BSM). White dotted line indicates the deep anal sphincter.

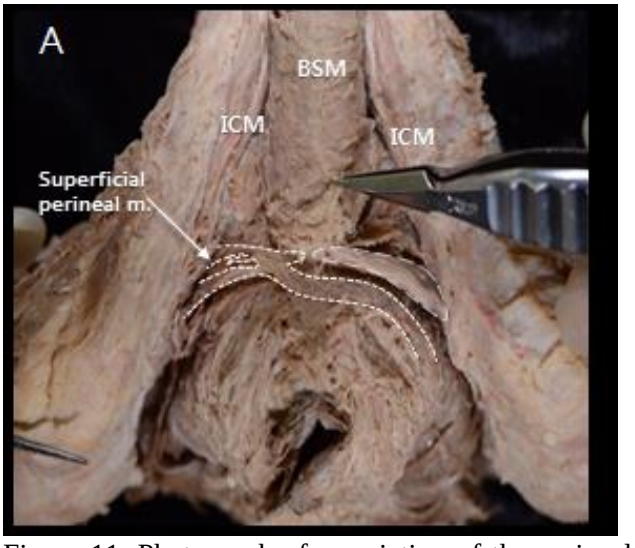

Figure 11. Photograph of a variation of the perineal body. The muscle fibers of the superficial perineal muscle and the superficial anal sphincter muscle fibers cross one another and connect.

The perineal body was absent in two samples. These samples did not have superficial transverse perineal muscles, but instead had accessory superficial muscles. The deep anal sphincter ran along the shaft and connected to the BCM on the lateral side of the shaft (Figure 12).

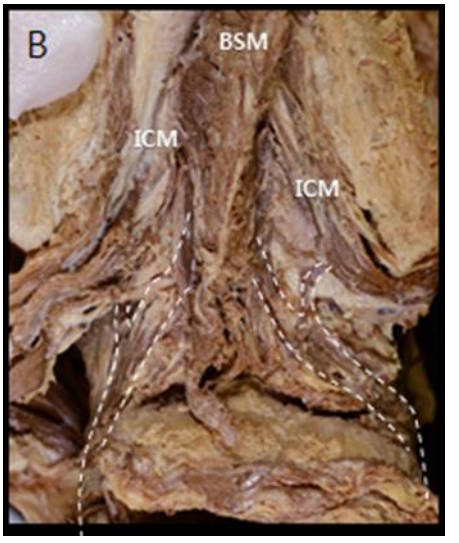

Figure 12. A photograph of a case in which the perineal body was not formed. The superficial transverse perineal muscle is missing, and an accessory superficial muscle runs along the shaft. The superficial anal sphincter of both sides (white dotted line) are connected to the bulbospongiosus muscle.

G. Deep perineal pouch

After removing the perineal membrane, we observed that the deep perineal muscle, deep perineal artery, and vein pudendal nerve passed through the deep perineal pouch via a narrow space. The muscles within the deep perineal pouch were not in the form of a fascia with the muscles aligned in a horizontal fashion, but were in the shape of a hoof, similar to the female compressor urethra muscle. The anterior side of the urethra was either short or wide. In the case of urethras with a wide anterior side, muscle fibers were also observed around the anterior side (Figure 13). The area located one-third of the distance from the anterior

side across which the urethra traveled was very short. Figure 14 depicts the dimensions of the deep perineal pouch.

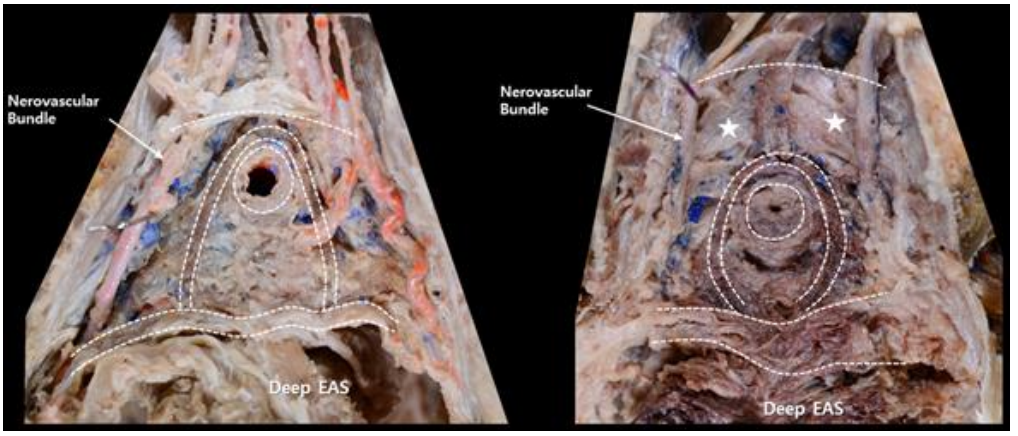

Figure 13. Photograph of the deep perineal pouch. The deep transverse perineal muscle is observed from the posterior side. A hoof-shaped muscle surrounds the urethra. The distance from the urethra to the anterior border was either (A) short or (B) long, in which case, muscle fibers were observed on the anterior side. (★)

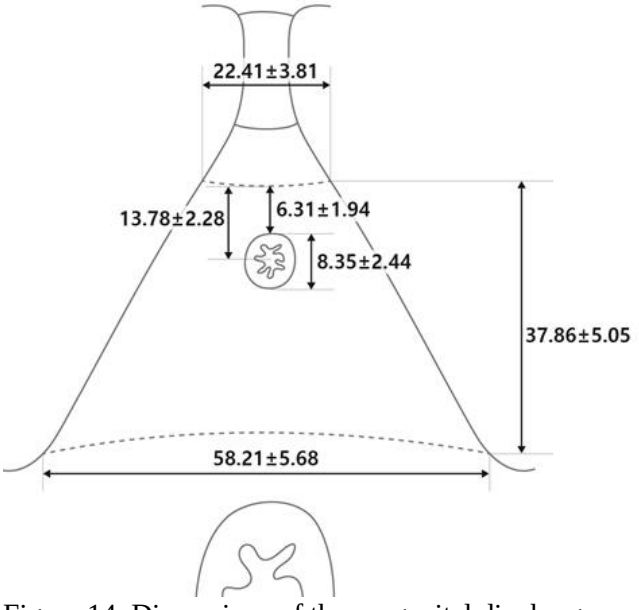

Figure 14. Dimensions of the urogenital diaphragm

3. Comparability of the 3D image

Three-dimensional reconstructions of the CT scans of the muscles of the urogenital diaphragm stained using the Lugol's staining technique were made, followed by another round of rendering. Surfaces of interest were selected and cropped step-by-step for structural observation. During image analysis, the individual layers and patterns of the muscles in the shallow layers were able to be visualized and analyzed in detail on the 3D images. However, because the muscles in the deep layers were thin and had various patterns, clear observation of their structures on the 3D images was limited.

IV. DISCUSSION

1. Puboprostatic ligament

The PPL was first reported to support the bladder neck and urinary continence following prostatectomy by Young.[25] The anatomical significance and structure of the PPL has been studied since then. Because the PPL is located in the innermost side of the narrow Retzius space, it is difficult to remove the prostate completely while preserving the PPL during open RP. While few publications have reported promising rates of urinary continence following PPL sparing radical prostatectomy[26,27], incomplete dissection of the apical margin, leading to high rates of positive surgical margins have also been reported.[28]

The space between the bilateral ligament is particularly important because the DVC passes through that area. In cases with one ligament, the distance was around 1 cm, but in cases with two ligaments it became narrower at approximately 6 mm. In cases with one ligament, the lateral wing was present in 55% of specimens, and the NVB pierced through the band. Thus, care should be taken not to perform blunt dissection in this area. The distance from NVB to the prostate is around 13 mm. Generally, an inverted v shape is formed as

approaching the prostate. In cases with more than two ligaments, the space became markedly narrow. These findings seem to be related to the size of prostate.

In 2014, Kim et al analyzed six cadavers and surgery videos of 300 RALRP and classified the PPLs into parallel, V shaped, inverted V shaped, and fused types. However, based on our observations, such classifications may be considered to be overly simplistic and not a true reflection of the actual shapes of PPLs. During surgery, it is very difficult to remove all the fat tissue, and clearly identify the 3D structures of the PPL. One important finding of this study is that double PPLs were found in 25% of all samples. By ignoring the type and number of PPLs, the risk of NVB injury is increased. If the surgeon is unaware of these potential variations, she or he could meet unexpected difficult situations during surgery. The PPLs are mostly located deep, in the lower third of the pubic bone. Type II and III PPLs are attached widely to the tendinous arcuate fascia. Thus, care should be taken during surgery not to injure the NVB or levator ani muscle to prevent urinary stress incontinence.

The hammock hypothesis proposed by DeLancy in 1997 presents a possible mechanism of urinary continence in women.[29] The hypothesis suggests that a hammock-like structure firmly supports the back of the urethra and increases abdominal pressure, which causes the urethra to collapse when the anterior wall becomes pressed, thereby preventing urinary incontinence. Men who undergo radical prostatectomy, are left with only the internal and external sphincter of the membranous urethra as structures that contribute to urinary continence, similar to female anatomy, in this regard. In the present study, the PPL was indeed observed to be firmly connected and fixed from the posterior side of the prostate to the bladder neck, further supporting the hammock hypothesis. A

midsagittal section of the samples showed the absence of a structure anterior to the membranous urethra that supports the urethra (Figure 15). Therefore, removal of the PPL in RP may increase the instability of the urinary bladder and urethra and negatively affect the recovery of urinary continence. The recently developed Retzius-sparing technique may minimize the risk of injury to the PPLs and NVB.

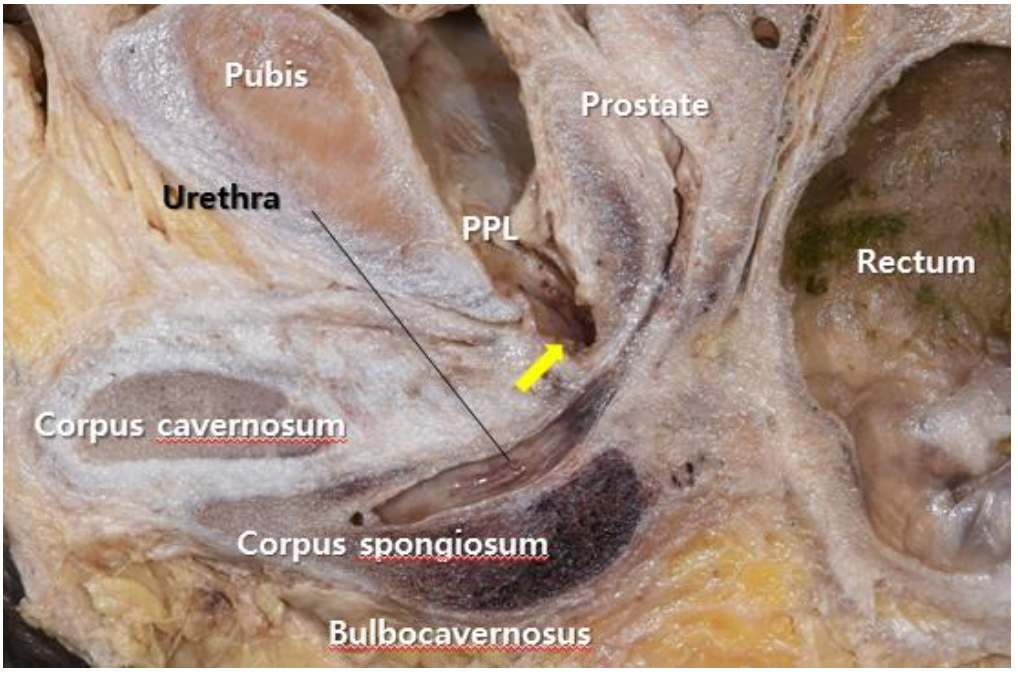

Figure 15. Midsagittal section. The yellow arrow indicates the anterior space of the urogenital diaphragm; PPl, puboprostatic ligament

2. Perineal structure

A. Cutaneous central band

Belt's approach is the preferred method for avoiding the urinary sphincter and urogenital diaphragm during perineal prostatectomy.[30] In this approach, the central tendon is identified as a landmark and the perineal body and superficial anal sphincter located behind it are then identified to approach the prostate.

However, only a few studies have reported which muscles the central tendon is attached to, as well as its morphology and function. Furthermore, the central tendon has commonly been confused with the the perineal body. In some atlases, the anatomic course of the central tendon is described as running horizontally[31], in others, the central tendon is said to be deeply located[32].

The first structure to appear when the skin of the perineum is removed was a fibrotic band that superficially connected the cutaneous anal sphincter with the BSM. This structure existed in layers that were more superficial than the perineal body, where the superficial perineal transverse muscle joins the BSM and superficial anal sphincter (Figure 5). In this study, the structure was observed in almost all samples; however, it was difficult to find the proper name of the structure or to search for previous studies conducted on it. We believe that this structure is an important landmark for surgery and thus requires a more distinct name and explanation of its anatomical location. Therefore, we have named the structure the 'cutaneous central band.' In 1999, Shafik reported that a medial fiber that originates from the anus runs along the corpus spongiosum down to the bulbar region, where it bifurcates to become the retractor penis muscle.[33] However, while we believe that the cutaneous central band plays a role in maintaining the location of the BSM, to a certain degree, our observations indicate that it is fibrotic and cannot be deemed to be a muscle. The mean distance from the BSM, which has this structure, and the anterior border of the external anal sphincter muscle is 15.8 mm, and this must also be taken into account. The cutaneous central band, which is the port of the traditional prostatectomy procedure, has received attention as a potential approach site for the new da Vinci robotic surgery technique. When performing a pudendal nerve block for urologic surgery, the ischial tuberosity and the cutaneous central band may provide a landmark for the selection of the optimal injection site.

B. Perineal Body

The perineal body (PB) is a fibromuscular structure that is the insertion site of six perineal muscles.[34] We confirmed that the perineal body was separated by deep and superficial PBs. We observed that the deep PB consisted of deep perineal muscles, and that the superficial PB consisted of superficial muscles. The deep PB was situated a slightly anteriorly, and we confirmed that these two bodies were connected. The PB has been reported to not exist.[35] In our study, we found that in two samples the fibers of the anal sphincter, superficial transverse muscle, and BSM were connected without passing through the PB. It is likely that the researchers in the earlier publication regarded these variations as evidence of an absence of the PB. The PB is connected to the anal sphincter with multiple muscle fibers and has a close relationship with the defecation function. During colorectal surgery, care should be taken not to injure this structure.

C. Accessory superficial transverse perineal muscle

The accessory superficial transverse perineal muscle is commonly observed in the superficial perineal pouch and includes the BSM, STPM, and ICM. In this study, an accessory muscle that did not belong to any of these three muscle types was observed in over 50% of all samples. This muscle was found bilaterally at the same time. The existence of this muscle has not been well documented, possibly because it is located between the ICM and the BSM and is hidden by these muscles. This accessory muscle may support the penis during erection and play a role in the elevation and backward retraction of the penis. Because it was found in 61.5% of samples, additional investigation on the functions of this accessory muscle is necessary and its significance should be assessed via

comparison with the compressor bulbar muscle, whose existence and functions are vaguely known.

D. Urogenital diaphragm

There have been conflicting reports regarding the morphology, constituent muscles, and even the existence of a deep perineal pouch with a urogenital membrane.[24] Several publications have described the muscles within this region as running horizontally; and some have reported the presence of a hoof-shaped structure resembling the female compressor urethra muscle, as well as a lack of membranes or diaphragm in these muscles.[36] There have also been reports that the external urethral sphincter muscle present in this region has a round shape[37] or omega shape.[38] Although the mean age of the cadavers used in this study was relatively old (79.6 years), we were able to observe the muscular urogenital diaphragm in all samples. We also observed that the muscles around the external sphincter surrounding the urethra was hoof shaped. The urethra was located in the proximal third of the urogenital diaphragm. We divided our samples into two groups according to the distance (short or long) from the anterior region of the urethra to the anterior border of the urogenital diaphragm. The samples in the short distance group had no muscles in the anterior region of the urethra and were unstably fixed in place (Figure 15). Therefore, if the PPL does not firmly fix the prostate, the urethra that passes through this region, as well as the urogenital diaphragm, is more susceptible to damage.

Urethral distraction injuries occur as the results of blunt pelvic trauma and are unique to the membranous urethra which is the weakest portion of urethra. However, the distraction can involve any portion of the membranous urethra between the departure of the BSM and the apex of the prostate.[39] Due to the distorted normal anatomic configurations, the surgeon should be armed with

profound knowledge about the anatomy of this deep pelvic area, to prevent the complications of incontinence and erectile failure during urethroplasty surgery.

3. Three-dimensional reconstruction image

It is challenging to studying the microanatomy of muscles with small volume and large variation, such as the perineum. Furthermore, obtaining tissue from samples, histological test results, and reconstructing them into 3D images is challenging and time consuming. We stained our samples with Lugol's solution (which has been used in animal studies) and preformed CT scans which we then reconstructed into 3D images. We investigated whether this procedure could replace histological analysis and actual dissection for studying the muscle layers. Metscher was the first to report the results of a study in which 3D CT using Lugol's solution was performed in 2009.[40] Since then, this technique has been used several times[41], however, most studies were experiments using animal samples. The only study that used a human sample was reported by Hutchinson et al. in 2016, in which the heart of a fetal cadaver was used.[42] The present study is the first in which the skeletal muscle of a relatively small mass (the perineum) was studied. This study confirmed the compatibility of 3D reconstruction images and real samples. We were able to accurately analyze the muscles of the superficial pouch and clearly observe the morphology, shape, and location using this technique, even without actual anatomic dissection. However, in the deep layers, it was challenging to analyze the muscles precisely due to the interindividual variations and also the non-continuity of the muscles. These results may be useful in the development of virtual training models. Ongoing development of 3D reconstruction of the human muscles is needed.

V. CONCLUSION

We observed varying types and morphologies of PPLs in the retropubic space. The PPL was confirmed to be an important structure that firmly holds and stabilizes the prostate. For the first time, we report an accessory superficial muscle which was observed in over 60% of all samples. It is necessary to study the functions of this muscle, which may include supporting the penis during erection and having a role in the elevation and backward retraction of the penis. The morphology of the deep transverse perineal muscle was not continuous, and both U and round shapes were observed. In 50% of samples, the front of the urethra was narrow and lacked a muscle. This indicates that it is necessary to review the anatomical importance of the PPL which firmly supports structures within the retropubic area. Surgery which preserves the PPL may prevent postoperative urinary incontinence.

REFERENCES

1. Cancer registry system in Korea. Available at http://www.ncc.re.kr
2. Myers RP. Practical surgical anatomy for radical prostatectomy. Urol Clin North Am 2001;28:473-90.
3. Myers RP, Cahill DR, Devine RM, King BF. Anatomy of radical prostatectomy as defined by magnetic resonance imaging. J Urol 1998;159:2148-58.
4. Di Pierro GB, Baumeister P, Stucki P, Beatrice J, Danuser H, Mattei A. A prospective trial comparing consecutive series of open retropubic and robot-assisted laparoscopic radical prostatectomy in a centre with a limited caseload. Eur Urol 2011;59:1-6.
5. Ficarra V, Novara G, Rosen RC, Artibani W, Carroll PR, Costello A, et al. Systematic review and meta-analysis of studies reporting urinary continence recovery after robot-assisted radical prostatectomy. Eur Urol 2012;62:405-17.
6. Bianco FJ, Scardino PT, Eastham JA. Radical prostatectomy: long-term cancer control and recovery of sexual and urinary function ("trifecta"). Urology 2005;66:83-94.
7. Stolzenburg JU, Kallidonis P, Do M, Dietel A, Hafner T, Rabenalt R, et al. A comparison of outcomes for interfascial and intrafascial nerve-sparing radical prostatectomy. Urology 2010;76:743-8.
8. Coakley FV, Eberhardt S, Kattan MW, Wei DC, Scardino PT, Hricak H. Urinary continence after radical retropubic prostatectomy: relationship with membranous urethral length on preoperative endorectal magnetic resonance imaging. J Urol 2002;168:1032-5.
9. Freire MP, Weinberg AC, Lei Y, Soukup JR, Lipsitz SR, Prasad SM, et al.

Anatomic bladder neck preservation during robotic-assisted laparoscopic radical prostatectomy: description of technique and outcomes. Eur Urol 2009;56:972-80.

10. Lee DI, Wedmid A, Mendoza P, Sharma S, Walicki M, Hastings R, et al. Bladder neck plication stitch: a novel technique during robot-assisted radical prostatectomy to improve recovery of urinary continence. J Endourol 2011;25:1873-7.
11. Coughlin G, Dangle PP, Patil NN, Palmer KJ, Woolard J, Jensen C, et al. Surgery Illustrated--focus on details. Modified posterior reconstruction of the rhabdosphincter: application to robotic-assisted laparoscopic prostatectomy. BJU Int 2008;102:1482-5.
12. Hurtes X, Roupret M, Vaessen C, Pereira H, Faivre d'Arcier B, Cormier L, et al. Anterior suspension combined with posterior reconstruction during robot-assisted laparoscopic prostatectomy improves early return of urinary continence: a prospective randomized multicentre trial. BJU Int 2012;110:875-83.
13. van der Poel HG, de Blok W, Joshi N, van Muilekom E. Preservation of lateral prostatic fascia is associated with urine continence after robotic-assisted prostatectomy. Eur Urol 2009;55:892-900.
14. Ploussard G, de la Taille A, Moulin M, Vordos D, Hoznek A, Abbou CC, et al. Comparisons of the perioperative, functional, and oncologic outcomes after robot-assisted versus pure extraperitoneal laparoscopic radical prostatectomy. Eur Urol 2014;65:610-9.
15. Galfano A, Ascione A, Grimaldi S, Petralia G, Strada E, Bocciardi AM. A new anatomic approach for robot-assisted laparoscopic prostatectomy: a feasibility study for completely intrafascial surgery. Eur Urol 2010;58:457-61.

16. Galfano A, Di Trapani D, Sozzi F, Strada E, Petralia G, Bramerio M, et al. Beyond the learning curve of the Retzius-sparing approach for robot-assisted laparoscopic radical prostatectomy: oncologic and functional results of the first 200 patients with >/= 1 year of follow-up. Eur Urol 2013;64:974-80.
17. Lim SK, Kim KH, Shin TY, Han WK, Chung BH, Hong SJ, et al. Retzius-sparing robot-assisted laparoscopic radical prostatectomy: combining the best of retropubic and perineal approaches. BJU Int 2014;114:236-44.
18. Lee SE, Byun S-S, Hong SK, Lee HJ, Kim YJ, Chang IH, et al. Anatomical Analysis of Prostate and Surrounding Structures: Points to Consider during Radical Retropubic Prostatectomy. Korean J Urol 2006;47:568-77.
19. Lee SE, Byun SS, Lee HJ, Song SH, Chang IH, Kim YJ, et al. Impact of variations in prostatic apex shape on early recovery of urinary continence after radical retropubic prostatectomy. Urology 2006;68:137-41.
20. Song C, Doo CK, Hong J-H, Choo M-S, Kim C-S, Ahn H. Relationship between the integrity of the pelvic floor muscles and early recovery of continence after radical prostatectomy. J Urol 2007;178:208-11.
21. Choi HM, Choi HK, Lee HY. Urinary Incontinence Could Be Controlled by an Inflatable Penile Prosthesis. World J Mens Health 2016;34:34-9.
22. Steiner MS. The puboprostatic ligament and the male urethral suspensory mechanism: an anatomic study. Urology 1994;44:530-4.
23. Kim M, Boyle SL, Fernandez A, Matsumoto ED, Pace KT, Anidjar M, et al. Development of a novel classification system for anatomical variants of the puboprostatic ligaments with expert validation. Can Urol Assoc J 2014;8:432-6.
24. Mirilas P, Skandalakis JE. Urogenital diaphragm: an erroneous concept casting its shadow over the sphincter urethrae and deep perineal space. J

Am Coll Surg 2004;198:279-90.

25. Young HH. The early diagnosis and radical cure of carcinoma of the prostate. Being a study of 40 cases and presentation of a radical operation which was carried out in four cases. 1905. J Urol 2002;167:939-46; discussion 47.
26. Poore RE, McCullough DL, Jarow JP. Puboprostatic ligament sparing improves urinary continence after radical retropubic prostatectomy. Urology 1998;51:67-72.
27. Deliveliotis C, Protogerou V, Alargof E, Varkarakis J. Radical prostatectomy: bladder neck preservation and puboprostatic ligament sparing--effects on continence and positive margins. Urology 2002;60:855-8.
28. Katz R, Salomon L, Hoznek A, de la Taille A, Antiphon P, Abbou CC. Positive surgical margins in laparoscopic radical prostatectomy: the impact of apical dissection, bladder neck remodeling and nerve preservation. J Urol 2003;169:2049-52.
29. DeLancey JO. The pathophysiology of stress urinary incontinence in women and its implications for surgical treatment. World J Urol 1997;15:268-74.
30. Belt E, Ebert CE, Surber A. A new anatomic approach in perineal prostatectomy. J Urol 1939;41:97.
31. Droller MJ. Surgical Management of Urologic Disease: Anatomic Approach. St. Louis: Mosby Year Book; 1992.
32. Hinman F. Atlas of urosurgical anatomy. Philadelphia: WB Saunders; 1993.
33. Shafik A. Physioanatomic entirety of external anal sphincter with bulbocavernosus muscle. Arch Androl 1999;42:45-54.
34. Shafik A, Sibai OE, Shafik AA, Shafik IA. A novel concept for the surgical

anatomy of the perineal body. Dis Colon Rectum 2007;50:2120-5.

35. Plochocki JH, Rodriguez-Sosa JR, Adrian B, Ruiz SA, Hall MI. A functional and clinical reinterpretation of human perineal neuromuscular anatomy: Application to sexual function and continence. Clin Anat 2016;29:1053-8.
36. Ricci J, Lisa J, Thom C. The female urethra: A histologic study as an aid in urethral surgery. Am J Surg 1950;79:499-505.
37. Oelrich TM. The urethral sphincter muscle in the male. Am J Anat 1980;158:229-46.
38. Strasser H, Klima G, Poisel S, Horninger W, Bartsch G. Anatomy and innervation of the rhabdosphincter of the male urethra. Prostate 1996;28:24-31.
39. Iselin CE, Webster GD. The significance of the open bladder neck associated with pelvic fracture urethral distraction defects. J Urol 1999;162:347-51.
40. Metscher BD. MicroCT for comparative morphology: simple staining methods allow high-contrast 3D imaging of diverse non-mineralized animal tissues. BMC Physiol 2009;9:11.
41. Gignac PM, Kley NJ, Clarke JA, Colbert MW, Morhardt AC, Cerio D, et al. Diffusible iodine-based contrast-enhanced computed tomography (diceCT): an emerging tool for rapid, high-resolution, 3-D imaging of metazoan soft tissues. J Anat 2016;228:889-909.
42. Hutchinson JC, Arthurs OJ, Ashworth MT, Ramsey AT, Mifsud W, Lombardi CM, et al. Clinical utility of postmortem microcomputed tomography of the fetal heart: diagnostic imaging vs macroscopic dissection. Ultrasound Obstet Gynecol 2016;47:58-64.

ABSTRACT (IN KOREAN)

미래의 전립선 수술을 위한 남성 치골뒤 공간과 비뇨생식 격막의 미세해부구조 및 3차원 영상의 효용성

<지도교수 이혜연>

연세대학교 대학원 의학과

최 현 민

I. 서론: 전립선 암이 조기 진단된 경우에는 근치적 전립선 적출술이 완치를 위한 가장 확실한 치료방법으로 추천이 되나 술 후 발기부전과 요실금의 합병증이 문제가 되어왔다. 이런 문제를 해결하기 위해 많은 술기적 발전들이 있어 왔으며 최근엔 치골 뒤 공간 보존 및 회음부를 통한 수술적 접근법 등의 방법이 관심을 받고 있다. 하지만 이러한 구조들에 대한 해부학적 연구가 많이 부족하며 논란이 있어왔다. 따라서 이 분야의 정확한 해부학적 구조를 연구하고 이해하는 것이 수술 술기 발전과 합병증 감소에 도움이 될 것으로 생각되어 본 연구를 진행하게 되었다.

II. 재료 및 방법: 연세대학교 의과대학에 유언하고 기증된 시신 중 관련부위의 수술 처치를 하지 않은 한국 성인 남자 시신 30구를 사용하였다. 6 구의 시신은 CT 촬영을 위한 루골 염색을 하였다. 통상의

방법으로 골반을 정리하여 치골전립선인대를 관찰하였으며 회음부의 얕은 샅공강, 샅힘줄중심, 깊은 샅공간의 구조를 순서대로 해부하여 관찰하였다. 루골로 염색한 표본은 통상의 CT 촬영 후 3차원 재구성하여 관찰하였으며 이후 해부를 진행하여 비교하여 보았다. 통계적 분석은 T 검정과 카이 스퀘어 검증을 사용하였다.

III. 결과: 치골전립선인대는 크게 4가지형태로 분류가 가능하였고 한쪽에 2개가 있는 경우도 25% 정도에서 관찰되었다. 붙는 위치는 치골의 하방 1/3의 매우 깊은 곳에 붙는 것을 확인하였으며 인대 사이의 거리는 평균 8.5mm 로 관찰되었다. 피부항문괄약근과 망울해면체근을 연결하는 피부 중심 띠가 있는 것을 관찰하였고, 보조 얕은샅 가로근의 존재도 처음으로 관찰하였다. 샅힘줄중심의 구조가 두 층으로 되어 있으며 서로 연결되어 있음을 관찰하였다. 깊은 샅공간에 요도를 말발굽 모양으로 감싸는 근육이 관찰되었고 요도로부터 앞쪽 경계까지 거리가 짧은 경우와 긴 경우로 구분되었으며 긴 경우엔 앞쪽에 근 섬유가 관찰되었다. 루골 염색 후 CT를 촬영한 것을 3차원으로 재구성한 후 구조를 관찰한 결과 얕은층의 근육들은 그 층과 결이 자세히 보여지며 분석이 가능한 것을 확인 할 수 있었다.

IV. 결론: 치골뒤 공간에서 치골전립선인대는 다양한 수와 형태로 관찰되었으며, 전립선을 단단히 붙잡아서 안정시키는 매우 중요한 구조임을 확인하였다. 60% 이상에서 관찰된 보조 얕은샅 가로근은 처음으로 보고하는 근육이며 발기 시 음경을 지지해 주며 발기시 음경을 위쪽으로 올려주며 뒤쪽으로 당겨주는 수축에 관여하는 역할을 하는 것으로 생각되

므로 그 기능에 주목할 필요가 있다. 깊은살 가로근의 형태는 연속적이지 않았으며, U자나 둥근 형태인 부분을 관찰하였다. 특히 요도 앞쪽 부분이 좁고 근육이 없는 경우가 50%였으며, 이 경우 치골뒤 공간에서 구조들을 단단히 지지해 주는 치골 전립선인대의 해부학적 중요성을 재조명할 필요가 있으므로, 이를 보존하는 수술법을 시행하는 것이 수술 후 요실금 등을 예방하는데 필요하다고 생각한다.

핵심되는 말 : 전립선 암; 치골전립선인대; 비뇨생식 격막; 3차원 재구성 영상

PUBLICATION LIST

1. Choi HM, Lee HY, Kim YT, Shin JC, Kim JH, Yang HJ, et al. Clinical Anatomy of the Puboprostatic Ligament for the Safe Guidance for the Prostate Surgery. Urology 2020;136:190-195.